

Osteogenesis Induced by Extracorporeal Shockwave in Treatment of Delayed Osteotendinous Junction Healing

Ling Qin,¹ Lin Wang,^{1,2} Margaret Wan-nar Wong,¹ Chunyi Wen,¹ Gang Wang,¹ Ge Zhang,¹ Kai-ming Chan,¹ Wing-hoi Cheung,¹ Kwok-sui Leung¹

¹Musculoskeletal Research Laboratory, Department of Orthopaedics and Traumatology, The Chinese University of Hong Kong, Shatin, N.T. Hong Kong SAR, China, ²Institute of Human Sports Science, Beijing University of Physical Education, Beijing, PR China 100084

Received 11 December 2008; accepted 8 June 2009

Published online 14 July 2009 in Wiley InterScience (www.interscience.wiley.com). DOI 10.1002/jor.20948

ABSTRACT: Healing at the osteotendinous junction (OTJ) is challenging in orthopedic surgery. The present study aimed to test extracorporeal shockwave (ESW) in treatment of a delayed OTJ healing. Twenty-eight rabbits were used for establishing a delayed healing (DH) model at patella-patellar-tendon (PPT) complex after partial patellectomy for 4 weeks and then were divided into DH and ESW groups. In the ESW group, a single ESW treatment was given at postoperative week 6 to the PPT healing complex. The samples were harvested at week 8 and 12 for radiographic and histological evaluations with seven samples for each group at each time point. Micro-CT results showed that new bone volume was $1.18 \pm 0.61 \text{ mm}^3$ in the ESW group with no measurable new bone in the DH group at postoperative week 8. Scar tissue formed at the OTJ healing interface of the DH group, whereas ESW triggered high expression of VEGF in hypertrophic chondrocytes at week 8 and regeneration of the fibrocartilage zone at week 12 postoperatively. The accelerated osteogenesis could be explained by acceleration of endochondral ossification. In conclusion, ESW was able to induce osteogenesis at OTJ with delayed healing with enhanced endochondral ossification process and regeneration of fibrocartilage zone. These findings formed a scientific basis to potential clinical application of ESW for treatment of delayed OTJ healing. © 2009 Orthopaedic Research Society. Published by Wiley Periodicals, Inc. *J Orthop Res* 28:70–76, 2010

Keywords: extracorporeal shockwave (ESW); osteotendinous junction; osteogenesis; delayed healing; partial patellectomy

Many orthopedic injuries involve surgical repair of musculoskeletal tissues around joints. Yet the surgical result is not always as expected, as delay in repair of musculoskeletal tissues may occur. Apart from delay in fracture repair,¹ the delayed healing at the osteotendinous junction (OTJ) is a more challenging situation after musculoskeletal injury. As shown in clinical biopsies at OTJ of the patellar tendon after graft harvesting in patients under knee reconstructive surgery, scar tissue formation with limited capability of remodeling at the healing OTJ prevented osteogenesis and regeneration of fibrocartilage zone at the healing interface.^{2,3}

For evaluating the potential treatment efficacy of biophysical modalities for treatment of difficult OTJ healing, the authors of the present study established a delayed OTJ healing model for the first time, creating a critical gap defect between patellar tendon and proximal patella after partial patellectomy, where massive scar tissue formation with a consistent delay in osteogenesis was demonstrated.⁴ Osteogenesis at the healing interface of the patella-patellar-tendon (PPT) complex after partial patellectomy has been reported to be associated with healing quality experimentally⁵ and clinically.⁶ Therefore, enhancement of osteogenesis in delayed OTJ healing would be essential for achieving better mechanical properties of the healing complex.

Both low-intensity pulsed ultrasound (LIPUS) and high energy extracorporeal shockwave (ESW) have been recently tested for treatment of chronic soft tissue

injuries, delayed fracture union and nonunion.^{7–12} One major advantage of ESW over LIPUS is its short (single or few treatment sessions) treatment regime, where ESW produces pressure waves that generate high positive pressures and cavitations at focal treatment regions of musculoskeletal tissues. The underlying mechanisms were reported to be effective to induce tissue micro-damage, triggering angiogenesis via up-regulation of vascular endothelial growth factor (VEGF),^{13,14} promoting chondrogenesis¹⁵ and osteogenesis via activation of osteoblasts.^{16–18}

The authors hypothesized that ESW could induce osteogenesis with triggering VEGF expression, promotion of endochondral ossification, and regeneration of fibrocartilage zone in delayed OTJ healing. In order to test this hypothesis, the present study was designed to evaluate angiogenesis, chondrogenesis, and osteogenesis with and without ESW treatment radiologically and histologically using an established delayed OTJ healing model in rabbits.

MATERIALS AND METHODS

Animals and Model Establishment

Twenty-eight mature female New Zealand rabbits (18 weeks old, $3.8 \pm 0.4 \text{ kg}$) were used for establishing the delayed OTJ healing at PPT complex after a standard partial patellectomy in one of the hind limbs using our recently established surgical protocol.⁴ Briefly, under general anesthesia with sodium pentobarbital (0.8 mL/kg, intravenous injection; Sigma Chemical Co., St. Louis, MO), a partial patellectomy was performed through a transverse osteotomy made between the proximal two-thirds and the distal one-third of the patella using an oscillating hand saw (Synthes; Mathys AG, Bettlach, Switzerland). After the distal third (lower pole) of the patella and its fibrocartilage zone to the patellar tendon were

Correspondence to: Ling Qin (T: 852-2632-3071; F: 852-2637-7889; E-mail: lingqin@cuhk.edu.hk)

© 2009 Orthopaedic Research Society. Published by Wiley Periodicals, Inc.

removed, two evenly spaced tunnels of 0.8 mm diameter were drilled longitudinally through the remaining proximal patella. Before the patellar tendon was sutured to the proximal patella via the two drilled holes with non-absorbable suture (3/0 Mersilk; Ethicon Ltd., Edinburgh, UK), a 3 × 2 mm rectangular latex sheet at a thickness of 1 mm (Ansell Medical, Victoria, Australia) was fixed between the remaining proximal patella and patellar tendon. Figure-of-8 tension band wiring (0.4 mm diameter stainless steel wire; Biomet Ltd., Waterton, UK) was applied around the proximal pole of the patella to the tibial tuberosity to protect overstretching of the suture for the junction reattachment before closing the wound. Cast immobilization was performed for the first 4 weeks. The latex slice was then surgically removed from the bone and tendon healing interface at the end of week 4. Animals were allowed free cage activities after surgery. Animal research ethics approval was obtained from the principal investigator's institution (Ref. No. CUHK4765/08). The institute's guidelines for the care and use of laboratory animals were followed.

ESW Treatment

The animals were quasi-randomized by using serial numbers assigned to the animal, with an odd number for ESW group ($n = 14$) and an even number for the delayed healing (DH) group with mock treatment ($n = 14$). Two weeks after removal of the immobilization cast and the interposed shielding sheet, the rabbits in the ESW group were sedated with ketamine (0.25 mL/kg, i.m.) for a single ESW treatment, with ESW delivered to the healing OTJ interface using a shockwave machine (Dornier MedTech Epos, Wessling, Germany). The treatment protocol composed of energy flux 0.43 mJ/mm² at a frequency of 4 Hz for 1,500 impulses, which was determined based on that established for achieving the optimal stimulatory effects for osteogenesis in our previous two *in vitro* studies.^{16,17} The ESW was delivered with a laser focus indicator and perpendicular to the healing interface of the proximal patella with knee flexion at 90° (Fig. 1).

Sequential Fluorescence Labeling

Sequential fluorescence labeling was used to study dynamic bone remodeling at the PPT healing complex using our established protocol.^{19–22} In brief, two fluorescent dyes, xylanol orange (90 mg/kg body weight) and calcein green (10 mg/kg body weight; both from Sigma-Aldrich GmbH), were injected subcutaneously and sequentially into the rabbits of the 8 week group at week 6 and 7 and of the 12 week group at week 10 and 11, postoperatively.

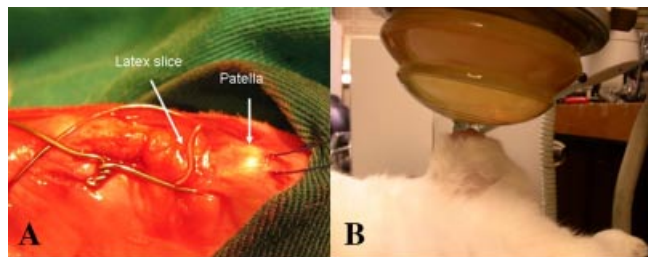


Figure 1. Delayed osteotendinous junction (OTJ) healing model and treatment. (A) Establishment of the delayed OTJ healing model. A latex slice (left arrow) was interposed for shielding the healing taking place at patellar tendon and patella (right arrow) for the first 4 postoperative weeks. (B) A single ESW treatment was given to the osteotendinous reattachment region at week 6 postoperatively.

Sampling and Evaluation

Fourteen rabbits of each group were euthanized at postoperative week 8 and 12 ($n = 7$ for each group and time point). The PPT complex of the operated knee was harvested for subsequent radiological and then histological evaluations.

Micro-CT Evaluation

Newly formed bone (NB) was evaluated using a high resolution micro-CT (micro-CT-40; Scanco Medical, Brüttisellen, Switzerland). In brief, the samples were placed with their long axes in the vertical position and immobilized with a foam pad in a cylindrical sample holder. The continuous scans were prescribed perpendicular to the long axis of the PPT complex at an isotropic resolution of 20 μm³. A total of 250 slices of each sample were scanned. The acquired 3D data set was first convoluted with a 3D Gaussian filter with a width and support equal to 1.2 and 2, respectively. Bone was segmented from the marrow and soft tissue for subsequent analyses using a global thresholding procedure. A threshold equal to or above 210 represented bone tissue; a threshold below 210 represented bone marrow and soft tissue according to our previous published work.^{20,22} The region of interest (ROI) of the NB was separated from the pre-existing bone by the osteotomy site at the remaining patella (Fig. 2). Bone mineral density (BMD), tissue volume (TV), and the fraction of bone volume (BV/TV) were measured.

Bone Histomorphometry

After micro-CT scanning, the specimens of the PPT complex were cut in half at midsagittal plane. One half was embedded in methylmethacrylate (MMA) without decalcification for fluorescence microscopic examination and the other half was decalcified for morphological evaluation. The MMA specimens

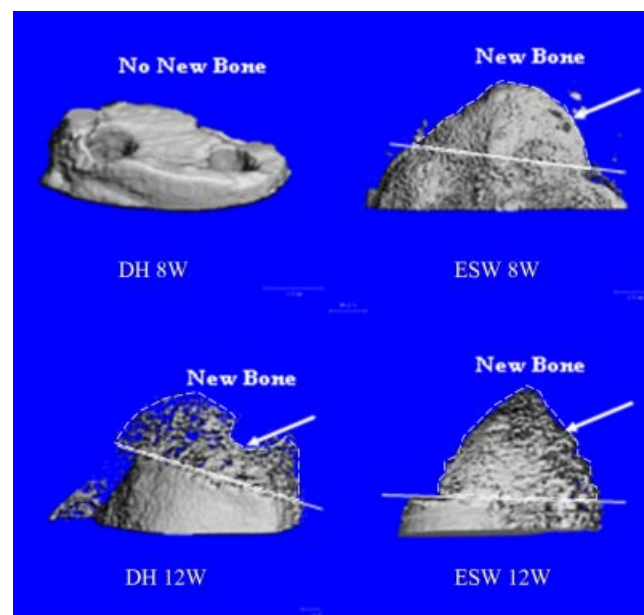


Figure 2. Representative micro-CT reconstruction of new bone delineated by dotted line (arrows) formed at the patella-patellar tendon complex healing interface compared between the delay healing group (DH) and the ESW treatment group (ESW). The newly formed bone of the ESW group at both week 8 (ESW 8) and week 12 (ESW 12) was more than that of the DH group at both week 8 (DH 8W) and week 12 (DH 12W), respectively. The white line overlays the osteotomy bony interface separating the residual proximal patella and the new bone.

were cut sagittally at a thickness of 200 μm using a saw microtome (SP 1600; Leica, Germany) and then polished to 80–100 μm by a polisher (RotoPol-21; Struers, Denmark) before digitalization using a fluorescence microscopic system (Leica Q500MC; Leica Cambridge Ltd., Cambridge, UK). The mineral apposition rate (MAR) was measured using MetaMorph Image Analysis System 6.3 (Universal Imaging Corp.; Molecular Devices, Downingtown, PA).

Morphological Evaluation

The decalcified specimens were embedded in wax. Sections (7 μm thick) were cut along the sagittal plane of the PPT complex and stained with Hematoxylin-Eosin (H&E) for microscopic examination. The cell density of fibrocartilage and fibrous tissue was evaluated respectively; the area of fibrocartilage zone was also measured using an established protocol.^{23,24} The healing quality at OTJ healing interface was graded morphologically using Yamakado's method,²⁵ with no interface tissue regeneration (score = 0), indirect integration with scar tissue (score = 1), direct integration with collagen fiber reconnection (score = 2), and regeneration of fibrocartilage zone (score = 3).

Immunohistochemical Evaluation

The expression of VEGF at the OTJ healing interface was examined via immunohistochemical staining using our established protocol.²³ Briefly, after removal of paraffin and dehydration, consecutive paraffin sections from each sample were quenched with 0.5% hydrogen peroxide for 20 min, and transferred to 10 mmol/L citrate buffer solution (pH 6) and boiled in a microwave (700 W) oven for 1 min. After brief digestion with 0.05% trypsin for 5 min and neutralization with 1% bovine serum albumin in phosphate buffered saline for 20 min, the sections were incubated with primary antibody in a humid chamber at 4° overnight. Mouse monoclonal antihuman VEGF antibodies were used at a dilution of 1:500. Negative stain controls were prepared by omitting the primary antibody. After thorough washing with phosphate buffered saline, the sections were incubated with biotinylated antimouse IgG antibody (DAKO, Glostrup, Denmark). The classic antibody binding complex method was used to amplify the specific binding signal (DAKO). Finally, 3, 3'-diaminobenzidine tetrahydrochloride was used to develop color in the presence of H_2O_2 . The sections were rinsed in distilled water, counterstained in Mayer's Haematoxylin, dehydrated through graded alcohol to xylene, and mounted with *p*-xylene-bis-pyridinium bromide (DPX) (Sigma, Aldrich) coated slides. The light microscopic examinations were then performed. The percentage of VEGF-positive cell number over total cell number was calculated in five rectangular areas (100 \times 100 μm^2) at the OTJ healing interface using an established protocol²³; the average of these five regions was used for statistical comparison.

Statistical Analysis

As new bone formation was not measurable under micro-CT and histological evaluations in DH group at postoperative week 8 (refer to Fig. 2), it was not included for statistical analysis. The comparisons for BMD, TV, BV/TV, and MAR were performed between ESW group of postoperative weeks 8 and 12 and the DH group of postoperative week 12 using independent measures *t*-test. The comparisons for histomorphometric data were performed using Mann-Whitney test. The level of significance was set at $p < 0.05$. All data analyses

were performed using SPSS 15.0 analysis software (SPSS Inc., Chicago, IL).

RESULTS

Micro-CT Evaluation

NB was obvious in the experimental group as compared with no measurable NB of the DH group at postoperative week 8 (Fig. 2). The volume of NB in the ESW group at both week 8 and 12 did not differ from that of DH group at week 12 after surgery. But the fraction of NB of the ESW group at both postoperative week 8 and 12, which was indicated by BV/TV, was significantly higher than that of the DH group at week 12 postoperatively. BMD in the ESW group at both week 8 and 12 was significantly higher than that of the DH group at week 12, postoperatively (Table 1).

Sequential Fluorescence Labeling

Under fluorescence microscopic evaluation, NB of the DH group was not evident at week 8 but quantifiable at week 12 after surgery as compared with the obvious NB formation in the ESW group at both week 8 and 12 after surgery (Fig. 3). The MAR of NB in the ESW group at both week 8 and 12 was significantly higher than that of the DH group at week 12 after surgery (Table 1).

Morphological Evaluation

In the DH group, there was extensive fibrous tissue formation with a distinct boundary at the initial osteotomy site at postoperative week 8 (Fig. 4A). The fibrous interface was characterized by hypercellularity with cigarlike and round cells, and poor collagen fiber organization and alignment. At postoperative week 12, new bone formation was present at the OTJ healing interface with re-establishment of collagen fiber connection from bone to tendon (Fig. 4C). As shown in Table 1, the cell density of fibrous interface decreased in the ESW group at each healing time point ($p < 0.05$).

After ESW treatment, cartilaginous tissue was present at the OTJ healing interface at postoperative week 8 (Fig. 4B); with healing over time, the tidemark in the regenerated fibrocartilage zone appeared at the OTJ healing interface at postoperative week 12 (Fig. 4D). The chondrocytes, morphologically characterized by round nucleus in lacuna, were embedded in organized and aligned collagen fibers, which were made up of fibrocartilaginous interface. As shown in Table 1, the decrease of fibrocartilage zone and cell density was accompanied by an increase in new bone formation. It was noted that the cell density at the healing interface was significantly lower after ESW treatment as compared with that in the DH group.

The OTJ healing quality of the ESW group at both postoperative week 8 and 12 was significantly better, with regeneration of fibrocartilage zone and direct tendon-to-bone collagen fiber reconnection, than that of the DH group with fibrous interface at the OTJ at postoperative week 12 (Table 1).

Table 1. Comparison of Healing Characteristics at Osteotendinous Junction between DH and ESW Group

Healing Characteristics at Osteotendinous Junction	Grouping			
	DH week 8 (n = 7)	ESW week 8 (n = 7)	DH week 12 (n = 7)	ESW week 12 (n = 7)
Osteogenesis				
Newly-formed bone mineral density (mg/mm ³)	/	0.52 ± 0.18	0.35 ± 0.12	0.72 ± 0.15*
Newly-formed bone tissue volume (mm ³)	/	1.18 ± 0.61	1.61 ± 0.39	1.95 ± 1.24*
Newly-formed bone fraction (%)	/	15.45 ± 10.86*	3.51 ± 2.53	56.54 ± 30.43*
Mineral apposition rate ((µm/week)	/	1.50 ± 0.47*	0.94 ± 0.27	1.98 ± 0.75*
Chondrogenesis				
Area of fibrocartilage zone (mm ²)	0	0.32 ± 0.11 [#]	0	0.23 ± 0.09 [#]
Cell density of fibrocartilage (number/mm ²)	0	36 ± 5 [#]	0	22 ± 7 [#]
Cell density of fibrous tissue (number/mm ²)	136 ± 32	78 ± 19 [#]	94 ± 21	46 ± 11 [#]
Angiogenesis				
Percentage of VEGF-positive cells	19 ± 9%	48 ± 15% [#]	23 ± 7%	29 ± 13% [#]
The score of healing quality: median [range]	1 [0,1]	2 [2,3] [#]	1 [1,2]	3 [2,3] [#]

Note: "/": Newly-formed bone was not measurable under micro-CT at week 8 and it was not included for statistical analysis.

*Indicated the significance of the comparisons for the newly-formed bone mineral density and volume, and the mineral apposition rate between ESW group of week 8 and 12 and DH group of week 12 using independent-measures t-test. The level of significance was set at $p < 0.05$.

[#]Indicated the significance of the comparisons for histomorphometric data between ESW and DH group using Mann-Whitney test. The level of significance was set at $p < 0.05$.

Immunohistochemical Evaluation

In the ESW group, the immunoreactivity of VEGF signals was detected at the OTJ healing interface, which was highly expressed in hypertrophic chondrocytes in

the ESW group at postoperative week 8. The percentage of VEGF-positive cells decreased with healing over time, with maturation of healing interface tissue at OTJ at week 12 in the ESW group. The percentage of VEGF-positive cells was significantly higher after ESW treatment as compared with the DH group at both week

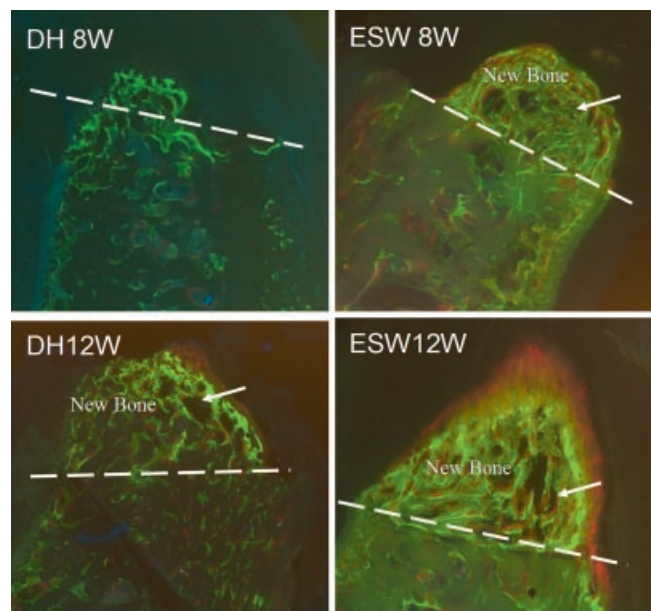


Figure 3. Representative micrographs show dynamic process of new bone formation at patella-patellar tendon complex healing interface compared between the delay healing group (DH) and ESW treatment group (ESW). The green and red labeling indicated mineral deposition of newly formed bone at weeks 6 and 7 of the week 8 (8W) groups and at weeks 10 and 11 of the week 12 (12W) groups. Massive mineral apposition of newly formed bone (arrow) above the osteotomy line of the patella (white dotted line) in the ESW group was shown at postoperative weeks 8 and 12. In contrast, the newly formed bone in the DH group was not obvious at postoperative week 8 but then became intense at week 12 in the DH group. Original magnification: 16×.

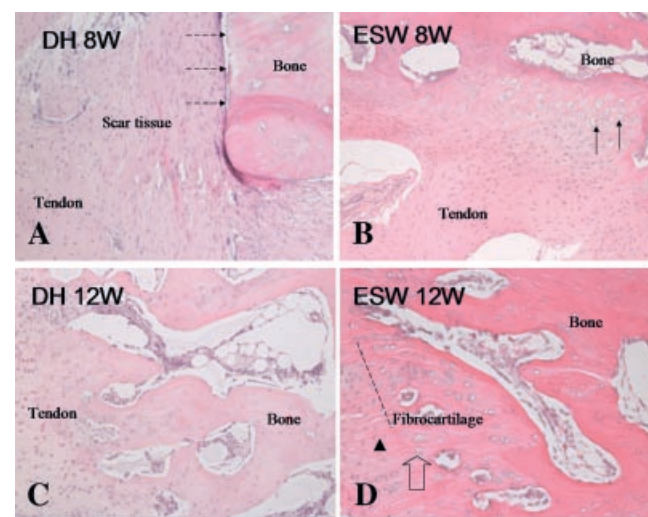


Figure 4. Representative histological features shown at the patella-patellar tendon complex healing interface compared between the delay healing groups (DH) and ESW treatment groups (ESW). (A,C) In the DH group, scar tissue formed at the healing interface with a distinct boundary between bone and tendon at the initial osteotomy site (arrow with dotted line) at postoperative week 8. The boundary became obscure, filling up with fibrous tissue with healing over time. (B,D) In the ESW group, transient fibrocartilage formation (arrow) was present at week 8 after surgery while the regeneration of fibrocartilage zone (black arrow) with tide mark formation (dotted line) and direct collagen fiber connection from bone to tendon (triangle) was found at week 12 in the ESW group. Magnification: 100×.

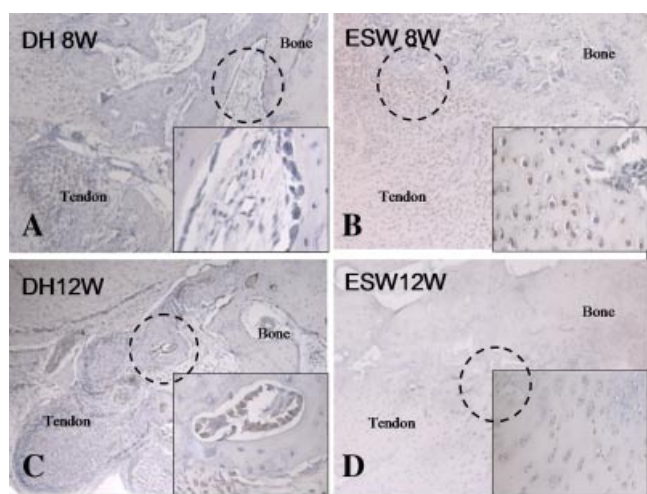


Figure 5. Representative histology of VEGF immunoreactivity at the patella-patellar tendon healing interface at both low (dotted circle) and high (box on the upper-right corner) magnifications compared between the delay healing groups (DH) and ESW treatment groups (ESW). (A,C) VEGF expression was low in the DH group at postoperative week 8 (A), but it was elevated at week 12, as detected in osteoblasts on the bone surface. (B,D) In contrast, the VEGF immunoreactivity of the ESW groups was evident in hypertrophic chondrocytes at the OTJ healing interface at week 8 and faded at week 12 after partial patellectomy (D). Low magnification: 50 \times . High magnification: 400 \times .

8 and 12 ($p < 0.05$ for both). In the DH group, VEGF expression was low at week 8 and slightly elevated at week 12 after surgery, which was expressed in osteoblasts lining along the bone surfaces at the healing interface of the healing OTJ (Fig. 5, Table 1).

DISCUSSION

The main findings of the present experimental study confirmed our study hypothesis that ESW could effec-

tively induce osteogenesis for treatment of delayed healing at OTJ in an established delayed OTJ healing model in rabbits. The new bone volume formed at the healing junction was utilized as the end-point for evaluation of treatment efficacy and repair quality,⁵ as more new bone formed at the OTJ healing interface was proven to be associated with better healing quality in terms of tensile strength of the PPT healing complex.^{5,26} The significantly enhanced osteogenesis in terms of new bone volume after a single ESW treatment regime revealed treatment efficacy for a delayed OTJ repair. In the present study, better healing quality was found after ESW treatment with regeneration of fibrocartilage zone at OTJ as compared with fibrous tissue in the DH group.

ESW accelerated the rate of OTJ healing as well as the improvement of healing quality. NB of the ESW group was present at postoperative week 8 whereas that of the DH group was noted after postoperative week 12. It was consistent with our fluorescence microscopic findings that the mineral apposition rate was increased after ESW treatment at both postoperative week 8 and 12 as compared with that of the DH group. The NB volume measured by micro-CT was still higher in the ESW group as compared with the DH group at postoperative week 12. However, such a difference did not reach statistical significance level due to a rather large variation in the ESW group. The possible explanations were the variations in the responses of the healing tissues to the ESW stimuli and the postoperative cage activities of animals.

The process of new bone formation induced by ESW treatment resembled endochondral ossification. The experimental studies of others and ours suggest that the immediate effect of ESW is micro-damage to the

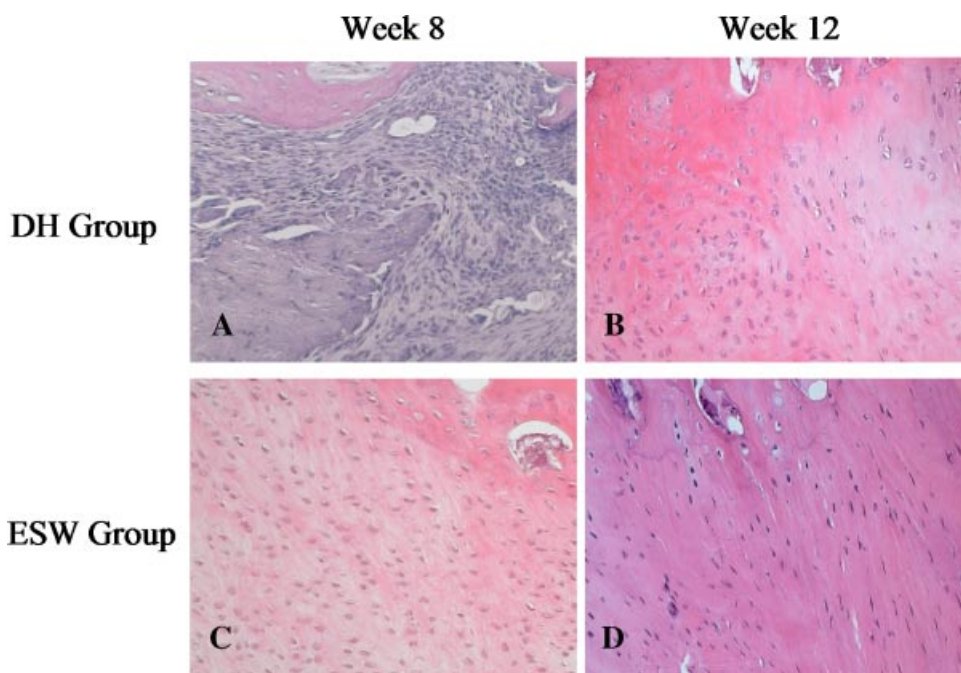


Figure 6. Representative histology showing the changes of tendon next to the healing OTJ in both delayed healing group (DH) (A,B) and ESW treatment group (ESW) (C,D) with healing over time. As compared with the DH group, the cell density of the healing tendon was significantly lower in the ESW treatment group at both postoperative weeks 8 (C) and 12 (D), suggesting advanced remodeling of the tendon matrix as compared with DH group. The change in cell morphology from round to spindle shaped also suggested the improved tendon function in the ESW group from week 8 (C) to week 12 samples (D) as compared with the DH group of the same healing time points. H&E staining. Magnifications: 200 \times .

cells,^{16,17} which subsequently triggers the up-regulation of the related extracellular cytokines and growth factors such as VEGF, BMP, and TGF- β .^{14,15} VEGF is not only essential for angiogenesis, but it is also involved in endochondral ossification.²⁷ As shown in the present study, VEGF is highly expressed in the hypertrophic chondrocytes, which are reported to be able to regulate the invasion of new blood vessels from the perichondrium and then subsequent degradation of the cartilage matrix.^{28,29} This is supported by the findings of the present study, which showed a decrease in the area of fibrocartilage zone and chondrocyte cell density. Other growth factors such as BMPs would also be influenced by ESW stimuli that are directly responsible for osteogenesis, apart from a up-regulated VEGF expression level found in the present study. It is known that the postnatal development process of OTJ also resembles endochondral ossification.³⁰ In the present study, ESW treatment was helpful for triggering the biological process towards restoration of the fibrocartilage zone in the delayed OTJ healing condition.

The stimulatory effect of ESW on a delayed OTJ repair was stage dependent with healing over time. In the early stage after ESW treatment, the cell density at the OTJ healing interface was significantly lower than that in the DH group, suggesting an advanced stage of tendon remodeling accompanied by a decrease in tendon cell numbers.^{16,17} ESW also triggered high VEGF expression in hypertrophic chondrocytes at the healing interface of OTJ. With the attenuation of VEGF immunoreactivity, the osteogenic effect of ESW emerged at postoperative week 12, showing an increase in the fraction of mineralized tissue from 15.45 to 56.54%. Our recent *in vitro* studies also revealed that ESW exerted its destructive effect in early stage and stimulatory effect in late stage.^{16,17} In the present study, ESW treatment was applied at postoperative week 6, instead of immediately after surgery or at postoperative week 4 after removal of the shielding. The findings in the present study only showed the beneficial effect of ESW treatment on a delayed healing at OTJ, but did not provide information on the optimal timing and dosage for the administration of ESW treatment. These issues need further investigation.

As compared with LIPUS, which requires daily treatment of 20 min and a few weeks to achieve treatment effects, only two to three treatments would be required for ESW, such as in the present study. This is more convenient and clinically applicable than daily treatment using LIPUS.^{31,32} Our recent *in vitro* and *in vivo* studies demonstrated that LIPUS exerted its beneficial effect only at an early stage of tissue healing.^{17,33} As ESW can be focalized onto the tissues sitting deep in the body, the expected beneficial effects to be generated from this study might also be generalized for treatment of delayed OTJ repair in other subcutaneous regions, such as hand, foot, ankle (e.g., Achilles-Calcanus), and shoulder (e.g., rotator cuff) in orthopedics.

There are a few limitations in the present study. As an outcome study, we were not able to delineate the underlying biological mechanisms of regeneration of bone-interface fibrocartilage zone and whether osteogenesis was from the bone marrow of the residual proximal patella or from the scar tissues formed at the OTJ healing interface after removal of distal patella after partial patellectomy, or from systemic circulating mesenchymal stem cells. Also, the optimal timing and dosage of ESW treatment were not determined in this study, but will be the subject of future studies. And finally, the histological evaluations were not conducted in a blinded fashion as the investigators of this study were also engaged in ESW intervention and subsequent radiographic monitoring of PPT interface healing, where we observed a statistically significant amount of new bone formation in the ESW group.

In conclusion, the findings of our experimental study suggested that ESW is a convenient and potential biophysical intervention for treatment of delayed OTJ healing, which we demonstrated radiologically and histologically. The potential clinical applications of ESW for treatment of complicated OTJ repair need further support of both experimental data and clinical evidence.

ACKNOWLEDGMENTS

This study was supported by the Research Grants Council of the Hong Kong Special Administrative Regions (Ref. CUHK4765/08). Histological preparations were made with the help of Miss Xiaohong Yang.

REFERENCE

- Green E, Lubahn JD, Evans J. 2005. Risk factors, treatment, and outcomes associated with nonunion of the midshaft humerus fracture. *J Surg Orthop Adv* 14:64–72.
- Liu SH, Hang DW, Gentili A, et al. 1996. MRI and morphology of the insertion of the patellar tendon after graft harvesting. *J Bone Joint Surg Br* 78:823–826.
- Sanchis-Alfonso V, Subias-Lopez A, Monteagudo-Castro C, et al. 1999. Healing of the patellar tendon donor defect created after central-third patellar tendon autograft harvest. A long-term histological evaluation in the lamb model. *Knee Surg Sports Traumatol Arthrosc* 7:340–348.
- Wang L, Qin L, Cheung WH, et al. 2008. A Delayed Bone-Tendon Junction Healing Model Established for Potential Treatment of Related Sports Injuries. *Br J Sports Med* (in press).
- Wang L, Lu HB, Cheung WH, et al. 2006. New bone formation and its size predicts the repair at patellapatellar tendon healing complex in rabbits. *J Med Biomech* 21:291–297.
- Saltzman CL, Goulet JA, McClellan RT, et al. 1990. Results of treatment of displaced patellar fractures by partial patellectomy. *J Bone Joint Surg Am* 72:1279–1285.
- Bara T, Synder M. 2007. Nine-years experience with the use of shock waves for treatment of bone union disturbances. *Orthop Traumatol Rehabil* 9:254–258.
- Gebauer D, Mayr E, Orthner E, et al. 2005. Low-intensity pulsed ultrasound: effects on nonunions. *Ultrasound Med Biol* 31:1391–1402.
- Schaden W, Fischer A, Sailer A. 2001. Extracorporeal shock wave therapy of nonunion or delayed osseous union. *Clin Orthop Relat Res* 387:90–94.

10. Rompe JD, Furia J, Maffulli N. 2009. Eccentric loading versus eccentric loading plus shock-wave treatment for midportion Achilles tendinopathy: a randomized controlled trial. *Am J Sports Med* 37:463–470.
11. Rompe JD, Meurer A, Nafe B, et al. 2005. Repetitive low-energy shock wave application without local anesthesia is more efficient than repetitive low-energy shock wave application with local anesthesia in the treatment of chronic plantar fasciitis. *J Orthop Res* 23:931–941.
12. Gerdesmeyer L, Wagenpfeil S, Haake M, et al. 2003. Extracorporeal shock wave therapy for the treatment of chronic calcifying tendonitis of the rotator cuff: a randomized controlled trial. *JAMA* 290:2573–2580.
13. Ma HZ, Zeng BF, Li XL. 2007. Upregulation of VEGF in subchondral bone of necrotic femoral heads in rabbits with use of extracorporeal shock waves. *Calcif Tissue Int* 81:124–131.
14. Chen YJ, Wurtz T, Wang CJ, et al. 2004. Recruitment of mesenchymal stem cells and expression of TGF-beta 1 and VEGF in the early stage of shock wave-promoted bone regeneration of segmental defect in rats. *J Orthop Res* 22:526–534.
15. Wang FS, Yang KD, Kuo YR, et al. 2003. Temporal and spatial expression of bone morphogenetic proteins in extracorporeal shock wave-promoted healing of segmental defect. *Bone* 32:387–396.
16. Tam KF, Cheung WH, Lee KM, et al. 2005. Delayed stimulatory effect of low-intensity shockwaves on human periosteal cells. *Clin Orthop Relat Res* 438:260–265.
17. Tam KF, Cheung WH, Lee KM, et al. 2008. Osteogenic Effects of Low-Intensity Pulsed Ultrasound, Extracorporeal Shockwaves and Their Combination—an in Vitro Comparative Study on Human Periosteal Cells. *Ultrasound Med Biol* 34:1957–1965.
18. Hofmann A, Ritz U, Hessmann MH, et al. 2008. Extracorporeal shock wave-mediated changes in proliferation, differentiation, and gene expression of human osteoblasts. *J Trauma* 65:1402–1410.
19. Qin L, Fok P, Lu H, et al. 2006. Low intensity pulsed ultrasound increases the matrix hardness of the healing tissues at bone-tendon insertion—a partial patellectomy model in rabbits. *Clin Biomech (Bristol, Avon)* 21:387–394.
20. Wen CY, Qin L, Lee KM, et al. 2009. Influence of bone adaptation on tendon-to-bone healing in bone tunnel after anterior cruciate ligament reconstruction in a rabbit model. *J Orthop Res* (in press).
21. Wen CY, Qin L, Lee KM, et al. 2009. The use of brushite calcium phosphate cement for enhancement of bone-tendon integration in an anterior cruciate ligament reconstruction rabbit model. *J Biomed Mater Res B Appl Biomater* 89:466–474.
22. Wen CY, Qin L, Lee KM, et al. 2008. Peri-graft bone mass and connectivity as predictors for the strength of tendon-to-bone attachment after anterior cruciate ligament reconstruction. *Bone* (in press).
23. Lu H, Qin L, Cheung W, et al. 2008. Low-intensity pulsed ultrasound accelerated bone-tendon junction healing through regulation of vascular endothelial growth factor expression and cartilage formation. *Ultrasound Med Biol* 34:1248–1260.
24. Wang L, Qin L, Lu HB, et al. 2008. Extracorporeal shock wave therapy in treatment of delayed bone-tendon healing. *Am J Sports Med* 36:340–347.
25. Yamakado K, Kitaoka K, Yamada H, et al. 2002. The influence of mechanical stress on graft healing in a bone tunnel. *Arthroscopy* 18:82–90.
26. Qin L, Leung KS, Chan CW, et al. 1999. Enlargement of remaining patella after partial patellectomy in rabbits. *Med Sci Sports Exerc* 31:502–506.
27. Dai J, Rabie AB. 2007. VEGF: an essential mediator of both angiogenesis and endochondral ossification. *J Dent Res* 86:937–950.
28. Rabie AB, Hagg U. 2002. Factors regulating mandibular condylar growth. *Am J Orthod Dentofacial Orthop* 122:401–409.
29. Rabie AB, Leung FY, Chayanupatkul A, et al. 2002. The correlation between neovascularization and bone formation in the condyle during forward mandibular positioning. *Angle Orthod* 72:431–438.
30. Rufai A, Benjamin M, Ralphs JR. 1992. Development and ageing of phenotypically distinct fibrocartilages associated with the rat Achilles tendon. *Anat Embryol (Berl)* 186:611–618.
31. Lu H, Qin L, Fok P, et al. 2006. Low-intensity pulsed ultrasound accelerates bone-tendon junction healing: a partial patellectomy model in rabbits. *Am J Sports Med* 34:1287–1296.
32. Qin L, Lu H, Fok P, et al. 2006. Low-intensity pulsed ultrasound accelerates osteogenesis at bone-tendon healing junction. *Ultrasound Med Biol* 32:1905–1911.
33. Fu SC, Shum WT, Hung LK, et al. 2008. Low-intensity pulsed ultrasound on tendon healing: a study of the effect of treatment duration and treatment initiation. *Am J Sports Med* 36:1742–1749.